

Modelling rogue waves through exact dynamical lump soliton controlled by ocean currents

Anjan Kundu,^{*} Abhik Mukherjee,[†] and Tapan Naskar[‡]
Theory Division, Saha Institute of Nuclear Physics
Kolkata, INDIA

Rogue waves are extraordinarily high and steep isolated waves, which appear suddenly in a calm sea and disappear equally fast. However, though the Rogue waves are localized surface waves, their theoretical models and experimental observations are available mostly in one dimension(1D) with the majority of them admitting only limited and fixed amplitude and modular inclination of the wave. We propose a two-dimensional(2D), exactly solvable Nonlinear Schrödinger equation(NLS), derivable from the basic hydrodynamic equations and endowed with integrable structures. The proposed 2D equation exhibits modulation instability and frequency correction induced by the nonlinear effect, with a directional preference, all of which can be determined through precise analytic result. The 2D NLS equation allows also an exact lump solution which can model a full grown surface Rogue wave with adjustable height and modular inclination. The lump soliton under the influence of an ocean current appear and disappear preceded by a hole state, with its dynamics controlled by the current term. These desirable properties make our exact model promising for describing ocean rogue waves.

PACS numbers: 02.30.lk, 92.10.H+, 02.30.jr, 42.65.Sf, 11.10.Lm, 47.35.Fg

Keywords: Nonlinear wave, integrable 2D NLS, exact lump soliton, rogue wave model, topological charge

1. INTRODUCTION

The mysterious ocean rogue waves (RWs) are reported to being observed in a relatively calm sea, where they, as a localized and isolated surface waves, apparently appear from nowhere, make a sudden hole in the sea just before attaining surprisingly high amplitude and disappear again without a trace [1–5]. This elusive freak wave caught the imagination of the broad scientific community quite recently [6–13], triggering off an upsurge in theoretical [5, 14–16] and experimental [3, 6–13] studies of this unique phenomenon. For identifying such extreme waves the suggested signature of these rare events is a deviation of the probability distribution function (PDF) of the wave amplitude from its usual random Gaussian distribution (GD), by having a long-tail, indicating that the appearance of high intensity pulses more often, has much higher probability than that predicted by the GD [17]. In conformity with this definition RWs were detected in a photonic crystal fiber [10], in a multi-stable state of an erbium doped fiber laser [13], in chaotic but deterministic regime of optical injected semiconductor lasers [3, 6], in nonlinear optical cavity [9], in acoustic turbulence in He II [7] and other set ups [11]. On the formation of the ocean RWs a number of supporting theories have been developed [2]. Among various possible factors contributing to the creation of the RW, the modulation instability (MI) supported by the nonlinear effect is believed to play a crucial role, by inducing preliminary amplification of water wave height, which may trigger self attractive nonlinear interaction, initiating the RW formation [18]. The MI can also cause wave-wave interaction leading to the four-wave mixing at matching frequencies and wave numbers, inducing resonance effect which might also develop into a RW [5, 11, 26]. Since the four-wave nonlinear interaction, a leading order nonlinear effect in deep-sea waves, is found also to be a dominant interaction in the nonlinear Schrödinger (NLS) equation

$$iq_t = q_{xx} + 2|q|^2q, \quad (1)$$

with the subscripts denoting partial differentiation, the NLS based nonlinear models are the most accepted ones for the RW, though often with certain modifications to include higher order dispersion or ocean currents, which are suspected to have a deciding role in the formation of the RW [4]. In extended space dimensional systems the nonlinear effect due to the MI in combination with a space-asymmetry, directional spectra and broken symmetry due to nonlocal coupling is suspected to be the major causes of such extreme waves [8, 9, 14]. The NLS equation (1) is a well known

evolution equation with integrability properties like having a Lax pair and exact soliton solutions [27]. Some models of RW generalize the NLS equation with the addition of extra terms on physical grounds, like ocean current [4], nonlinear dispersion [16, 28] etc. However such modifications of the NLS equation (1) make the system nonintegrable, allowing only numerical solutions. The most popular 1D RW model is a unique analytic rational solution of the original NLS equation (1) [19], given by the Peregrine breather (PB) [10, 12, 15] or its higher order versions [22]-[24] and the trigonometric variants [29, 30]. However, since the RW is an aperiodic event with a single appearance, the trigonometric breather solutions, due to their periodic nature, are not much suitable for a direct description of the RW. Nevertheless, interestingly these breather solutions, periodic in time [29] or in space [30], degenerate to the rational PB solution (2) at their periods going to infinity[33].

Note that the conventional soliton solution of the NLS equation (1), representing a localized translational wave behaves like a stable particle and unlike a RW propagates with unchanged shape and amplitude. Tsunami waves, though highly devastating, also exhibits different nature than the ocean RW. The ocean RW are deep sea waves with 2D character, localized in both space dimensions and appears as a single-peak event for a short interval of time. Tsunami waves on the other hand are manifested only in shallow water near the sea shore, though generated in the deep sea and propagate across a long distance. In the deep sea tsunami waves behave like 1D translatory wave, moving very fast with insignificant amplitude[20]. Therefore tsunamis and the RWs exhibit different features and dynamics and need different types of modelling which for the RW is still an open problem. More details on the progress in the study of the ocean RW can be found in some excellent reviews on the subject [2].

1.1. RW model on a 1D line

In contrast to the soliton or the trigonometric breather solutions of the NLS equation (1), its exact rational PB solution

$$q_P(x, t) = e^{-2it}(u + iv), \quad u = G - 1, \quad v = -4tG, \\ \text{where } G = 1/F(x, t), \quad F(x, t) = x^2 + 4t^2 + \frac{1}{4}, \quad (2)$$

represents a breather mode with unit amplitude at both distant past and future. The amplitude of the wave rises suddenly at $t = 0$, attaining its maximum at $x = 0$, though subsiding with time again to the same breathing state. This intriguing behavior makes the PB a popular candidate for the RW [10, 12, 15].

Since the characteristics of the envelop wave is the most significant in the description for the RW, the modulus of the PB solution (2)

$$|q_P(x, t)| = (u^2 + v^2)^{\frac{1}{2}} = [(G - 1)^2 + (4tG)^2]^{\frac{1}{2}}, \quad (3)$$

with G as in (2), is used in describing the RW profile. The full grown 1D RW at $t = 0$ therefore may be represented by

$$|q_P(x, 0)| = (G - 1)|_{t=0} = \left[\frac{1}{x^2 + \frac{1}{4}} - 1 \right], \quad (4)$$

as shown in Fig. 1. The maximum amplitude as seen from (4) is attained at $x = 0$ as $|q_P(0, 0)| = 3$. The modular inclination defined as

$$S_P^x(x) = \frac{\partial}{\partial x} |q_P(x, 0)| = -\frac{2x}{(x^2 + \frac{1}{4})^2} \quad (5)$$

attains its maximum $S_{Pmax}^x(x_m) = 3\sqrt{3}$ at $x_m = \pm \frac{1}{2\sqrt{3}}$.

Notice however that, the NLS equation (1) together with its different generalizations are equations in $(1 + 1)$ -dimensions and therefore all of their solutions, including the PB and its higher order generalizations, can describe the time evolution of a wave only along an one dimensional line (as in Fig. 1). Looking more closely into the PB we also

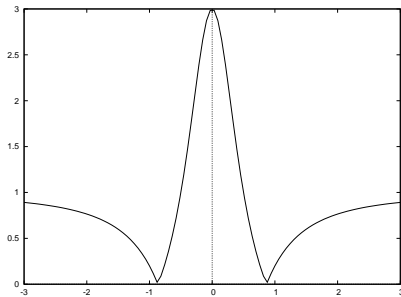


FIG. 1: Amplitude variation of the full grown 1D rogue wave, modelled by the modulus of the static Peregrine breather $|q_P(x, 0)|$. The maximum amplitude 3 is attained at $x = 0$, while it goes to its asymptotic value 1 at $x \rightarrow \pm\infty$. The maximum inclination attainable is $3\sqrt{3}$ at $x = \frac{\sqrt{3}}{6}$, and becomes 0 both at $x = 0$ and $x \rightarrow \pm\infty$.

realize that the maximum amplitude of this solution describing an 1D RW is fixed, and just three times that of the background waves (see Fig. 1). The modular inclination of this wave as well as the fastness of its appearance are also fixed, since solution (2) admits no free parameters. This situation can be improved to obtain higher amplitude and modular inclination of the PB model by using higher order rational solutions [22]. For example, the next higher order PB known also as Akhmediev-Peregrine breather can enhance the maximum wave elevation by a factor of five, while the next one by a factor of seven and so on, with an intriguing enhancement of factors by increasing odd numbers. Such increments in amplitude however are discrete and could be achieved at the cost of going to new solutions with increasingly complicated structures involving higher and higher order polynomials [22]. The maximum amplitude and modular inclination reachable by this class of solutions are fixed due to the absence of relevant free tunable parameters, making it difficult to adjust to the continuously varied range of shape and sizes of the observed oceanic RWs. However recently higher order rational solutions to the NLS equation allowing free parameters have been discovered [23, 24], though they seem to represent multi-peak wave in the $x - t$ plane for the nontrivial choice of parameters [24]. The single-peak solution which is suitable for describing RW having a single appearance in time, is obtained unfortunately for a trivial choice of the free parameters. The trigonometric breathers [29, 30] also contain free parameters [33], though such periodic solutions, as mentioned already, are different in nature than the single crest RW event. The crucial fact however is that, the 1D spatial nature remains the same for the whole class of the PB solutions, including its higher order rational and trigonometric generalizations. Therefore modelling an ocean RW, which is a 2D surface wave, by this class of 1D PB solutions remains problematic.

1.2. Need for a RW model on a 2D plane

Therefore, though the well accepted class of PB or other solutions of the generalized NLS equation could fit into the working definition of the ocean RW, saying any wave with height more than twice the nearby *significant height* (average height among one-third of the highest waves) could be treated as the RW [17], they perhaps, with their restricted characteristics, can explain successfully only fixed and moderately intense RW-like events on a 1D line, as observed in water channels [12], optical fibers [10, 13] or optical lasers [3, 6], but seem to be not satisfactory for modelling the ocean surface RWs.

Oceanic RWs are said to consist of an almost vertical wall of water preceded by a trough so deep, that it was referred to as a hole in the sea [25]. In march 2001, two reputed ships named as Bremen and Calendonian Star, carrying hundreds of tourists across the South Atlantic, had a devastating encounter with RW like events. It is reported by the witnesses that a giant isolated wave of around 30 meter high, fell upon the ship like a wall of water, out of no where and disappeared again without a trace [31]. At the initiatives of 11 organizations involving several countries in EU tasked the Earth - scanning satellites, named ERS-1 and ERS-2, to send images from a localized area of $10 \times 5 \text{ km}^2$ on the sea surface at certain locations to spot the possible occurrence of rogue waves [31].

All these available facts and information suggest that unlike the tsunami and internal waves, pictures of which can

be seen through satellite images [32], ocean RWs with the hole states must have a 2D character, localized in both the space dimensions. In 2D water basin experiments as well as in the related simulations the amplitude and the modular inclination of the RWs were found to be higher [8, 11, 14, 15] than those predicted and observed in 1D [12, 15].

The above arguments should be convincing enough to go beyond the 1D equations and search for a suitable (2+1) dimensional equations, to find a 2D alternative to the PB and other solutions of the 1D NLS equation, for constructing a more realistic model for the ocean RWs.

There are many nonlinear equations known in (2+1) dimensions having fruitful applications in various fields. Some of them allow exact analytic solutions, while others permit only approximate numerical simulation.

The well known KP equation is an integrable extension of the KdV equation to 2D space [44] describing the dynamics of a real field. However the KP equation like the KdV is a shallow water model, whereas the RW is naturally a deep water phenomenon.

There are also several equations extending the 1D NLS equation to (2+1) dimensions. From the basic hydrodynamic equations, by taking the perturbation analysis to a higher order, Dysthe has derived for the deep water waves a 2D evolution equation [33]. The Dysthe equation in general is non integrable .

The Davey-Stewartson equation [45] is an integrable generalization where the existence of rogue wave has been analyzed [42]. However such rogue wave solutions are reducible to the PB solution by a simple rotation in the plane. BLP equation [43] is another (2 + 1) dimensional integrable equation, defined through two real coupled equations. Recently a RW type solution has been found in this equation allowing a free parameter [48]. However since the BPL equation describes wave propagation along a channel , its applicability in modelling the ocean RW is questionable.

Zakharov have proposed several 2D equations, some of them are integrable [46, 47] while others are not [26]. Though these equations are applicable in other fields, the model proposed in [26] seem to be a successful model for the RW.

A straightforward 2D extension of the NLS equation :

$$iq_t = d_1 q_{xx} - d_2 q_{yy} + 2|q|^2 q, \quad (6)$$

where $q(x, y, t)$ is a slowly varying envelop and d_1, d_2 represents linear dispersion coefficients ([14]) of the deep water gravity wave, was proposed in connection with RW [14, 15].

Note however that the 2D NLS equation (6) is not an integrable system and gives only approximate numerical solutions with no stable soliton. Nevertheless, this unlikely candidate is found to exhibit RW like structures numerically, with higher amplitude and modular inclination and with an intriguing directional preference [8, 14] with broken spatial symmetry [9, 15]. However though the experimental and theoretical studies on nonlinear systems in 2D space have shown promises in describing more realistic situations in the formation of 2D ocean RWs, unfortunately, all of them can give only approximate numerical results and most of this models could not consider the effect of ocean current which is supposed to play a crucial role in the formation of ocean RWs [14, 15].

2. PROPOSED INTEGRABLE 2D NLS EQUATION

In the light of not so satisfactory present state in modelling the deep sea RWs, we propose an *integrable* extension of the 2D NLS equation:

$$iq_t = d_1 q_{xx} - d_2 q_{yy} + 2iq(\sqrt{d_1}j^x - \sqrt{d_2}j^y), \quad j^a \equiv qq_a^* - q^*q_a, \quad (7)$$

allowing an exact lump-soliton as a suitable RW model. In (7) the linear dispersion relation is exactly same as the conventional water wave dispersion as described in (6), with the only difference from this well known 2D NLS equation being in the nonlinear term. Notice that, when the conventional *amplitude*-like nonlinear term in the non-integrable equation (6) is replaced by a nonlinear *current*-like term (expressed through j_x, j_y), the resulting equation (7) miraculously becomes a completely integrable system with all its characteristic properties, which is much rarer in 2D than in 1D. Before proceeding further observe, that through scaling and a $\frac{\pi}{4}$ rotation on the plane : $(x, y) \rightarrow (\bar{x}, \bar{y})$ with $\bar{x} = \frac{1}{2}(-\frac{x}{\sqrt{d_1}} + \frac{1}{\sqrt{d_2}}y)$, $\bar{y} = \frac{1}{2}(\frac{x}{\sqrt{d_1}} + \frac{1}{\sqrt{d_2}}y)$ and $\bar{t} = 2t$, our 2D NLS equation (7) can be simplified to

$$iq_t + q_{xy} + 2iq(qq_x^* - q^*q_x) = 0, \quad (8)$$

where the *bar* over the coordinates is omitted. Encouragingly, our 2D NLS equation (8), at par with the well known 1D NLS equation is derivable from the more fundamental hydrodynamic equations and exhibits MI together with a nonlinear frequency correction, as we show below. Equation (8) admits also exact soliton and breather solutions through the standard formalism of Hirota's bilinearization and an associated Lax pair as well as an infinite set of conserved charges [35], proving thus the integrability of this nonlinear equation. More satisfactorily, equation (8), as we see below, admits an exact 2D generalization of the PB with the desirable properties of a realistic surface RW. It is promising that many characteristic properties like directional preference, MI, appearance of higher amplitude etc observed theoretically and experimentally in connection with the formation of RW in 2D models [8, 9, 14, 15], which remained as numerical approximations, get confirmed through analytic result in our model based on the integrable equation (8).

2.1. Nonlinear frequency correction and modulation instability

Instability of a planer wave, appearing due to the interplay between dispersion and nonlinear effect called Benjamin Feir or MI [40], which has been in the continuous focus for many years [38, 39], has gained more importance recently in the context of the RW. The nonlinearity and the MI are supposed to be the basic reason behind the formation of RWs. Therefore, before progressing further with our 2D NLS equation (8), we focus on the correction of its linear frequency induced by the nonlinear effect and the appearance of the MI mediated by such nonlinearity in the system. For investigating the contributions to the frequency due to the linear dispersive and the nonlinear term in (8), we insert the plane wave solution $q_0 = A_0 e^{i(\omega t + k^x x + k^y y)}$, with A_0 as the real constant amplitude, ω as frequency and (k^x, k^y) as the wave vector. For the plane wave to be an exact solution of (8), the frequency should be $\omega = \omega_L + \omega_{NL}$, $\omega_L = -k^x k^y$, $\omega_{NL} = 4A_0^2 k^x$, where ω_L is the frequency due to linear dispersion and ω_{NL} is its nonlinear correction, which depends on the amplitude of the wave as well as on the x component of the wave vector.

Now to explore the onset of MI in the system affecting this plane wave solution, we perturb it by a small parameter function $\epsilon(x, y, t)$. Note that the perturbation is considered in both the space directions since its importance in the instability in 2D is emphasized in the context of RW formation [15]. The solution

$$q_\epsilon = (A_0 + \epsilon) e^{i(\omega t + k^x x + k^y y)}, \quad (9)$$

neglecting the higher order terms in ϵ yields from (8) a linear equation for ϵ as

$$i\epsilon_t + \epsilon_{xy} + i(k^y \epsilon_x + k^x \epsilon_y) + 2iA_0^2(\epsilon_x^* - \epsilon_x) + 4A_0^2 k^x (\epsilon^* + \epsilon) = 0. \quad (10)$$

The appearance of the last two terms in equation (10) is due to the nonlinearity. For detecting the instability of the perturbation we represent $\epsilon = c_1 e^{i(\omega_m t + k_m^x x + k_m^y y)} + c_2 e^{-i(\omega_m t + k_m^x x + k_m^y y)}$. Inserting this form of perturbation in equation (10) and arranging the independent terms we get a set of two homogeneous equations for the arbitrary coefficients c_1, c_2 , nontrivial solutions of which can exist only when the determinant of the matrix vanishes leading to the necessary relation $\bar{\omega}_m^2 = K^2 - \Omega_c$, where $\bar{\omega}_m = \omega_m - \omega_0$, and $\omega_0 = 2A_0^2 k_m^x - k^x k_m^y - k_m^x k^y$, $K = k_m^x k_m^y - 4A_0^2 k^x$, $\Omega_c = 4A_0^4(4k^{x2} - k_m^{x2})$, which gives finally

$$\omega_m = \omega_0 \pm i\omega_I, \quad \omega_I = (\Omega_c - K^2)^{\frac{1}{2}}. \quad (11)$$

Therefore, under the condition $K^2 < \Omega_c$ with $\Omega_c > 0$, i.e when $|k_m^x| < 2|k^x|$ the modulation frequency ω_m can acquire an imaginary part ω_I , initiating an exponential growth of perturbation with time t and hence onsetting the MI. ω_I is the growth rate of the instability given by (11), a graphical form of which is presented in Fig. 2, showing its dependence on the longitudinal and transverse directions through k_m^x , and k_m^y respectively.

The stability plot is drawn in Fig. 3 in the (k_m^x, k_m^y) plane with the shaded region showing the domain of MI.

Both these figures show clearly, that the behavior of MI as well as the growth rate has a strong directional preference and range as observed also earlier in 2D models [8, 14, 15]. We have confirmed such properties through exact analytic result showing explicitly that in the MI as well as in the growth rate the components (k_m^x, k_m^y) of the wave vector do not enter symmetrically, in addition with a directional range $|k_m^x| < 2|k^x|$.

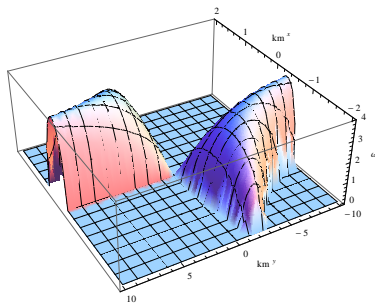


FIG. 2: The growth rate ω_I of the MI given by (11), arising in our 2DNLS equation, exhibiting how it changes (for $A_0 = 1.0, k^x = 1.0$) along the longitudinal (k_m^x) and transverse (k_m^y) directions, showing a strong directional preference.

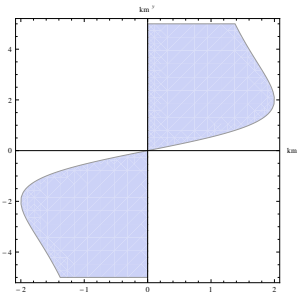


FIG. 3: Graphical representation of the MI region, where the instability can occur only within the shaded area (for fixed values of $A_0 = 1.0, K^x = 1.0$). The instability region, showing dependence on the wave vector (k_m^x, k_m^y) , varies asymmetrically along the longitudinal and transverse direction, as seen clearly from the figure.

A comparison here with the analysis of MI in case of the known 1D NLS equation [21] may be illuminating. The condition for the onset of instability in the 1D case involves only the nonlinear amplitude A_0 expressed in the form $|k_m^x| < 2A_0$, while in the present situation the condition is more complicated involving all components k_m^x, k_m^y, k^x apart from A_0 , together with an allowed range on the wave vector component, as found above analytically and shown graphically in Fig. 3. Similar situation is also true for the growth rates, where in the 1D case it is given by $\omega_I = |k_m^x|[(2A_0)^2 - (k_m^x)^2]^{\frac{1}{2}}$ [21], while in the present case the form of ω_I is more complicated and depends on both longitudinal and transverse directions, as shown above.

Thus the overall picture for the onset of the MI is similar to that occurring in the 1D NLS equation [21], though in the case of the 2D NLS equation (8) the details are different and more intricate with a directional preference and range, as seen also for the MI, initiating RW formation in some other systems in higher space-dimensions [8, 9, 14, 15]. We emphasize however, that in place of approximate numerical result obtained earlier, we found here similar properties in exact analytic form in our model. This is a strong point of our exact model. As in the case of the well studied 1D NLS model, we may expect the MI to play a key role in the creation of RWs based on our 2D NLS model (8).

3. MODELLING OF 2D ROGUE WAVES

Apart from finding a novel 2D integrable equation (8), our aim, relevant to the present problem, is to construct a 2D RW model as an exact solution of this equation.

3.1. Static lump soliton

Before presenting the dynamical lump solution related to (8) we consider first its static 2D lump-like structure:

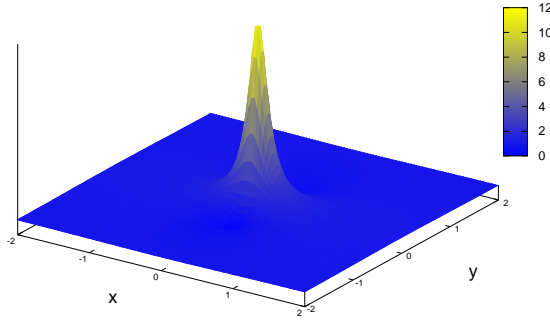
$$q_{P(2D)}(x, y) = e^{4iy}(u + iv), \quad u = G - 1, \quad v = -4yG, \\ \text{where } G \equiv \frac{1}{F(x, y)}, \quad F(x, y) = \alpha x^2 + 4y^2 + c, \quad (12)$$

localized in both space directions and describing a fully developed RW. One can check by direct insertion that (12), having two arbitrary parameters α and c , is an exact static solution of the 2D nonlinear equation (8). Solution (12), in spite of its close resemblance with the well known PB solution (2), marks some important differences. The static wave profile $|q_P(x, 0)|$ (4), obtained from PB solution (2) (see Fig. 1) at time $t = 0$ is a curve, representing full blown 1D RWs admitting no free parameters of relevance. On the other hand

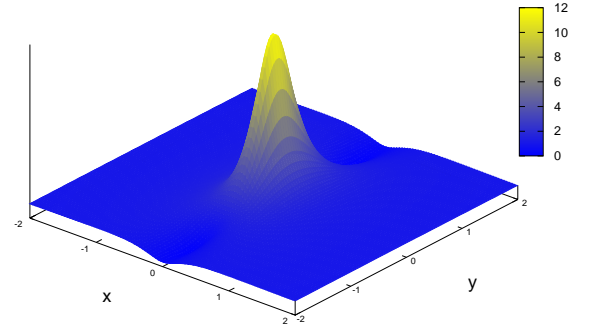
$$|q_{P(2D)}(x, y)| = (u^2 + v^2)^{\frac{1}{2}} = [(G - 1)^2 + (4yG)^2]^{\frac{1}{2}}, \quad (13)$$

obtained from the static solution (12) represents a 2D lump (see Fig. 4) with two independent free parameters, significance of which will be explained below and shown in Fig. 4(a-d).

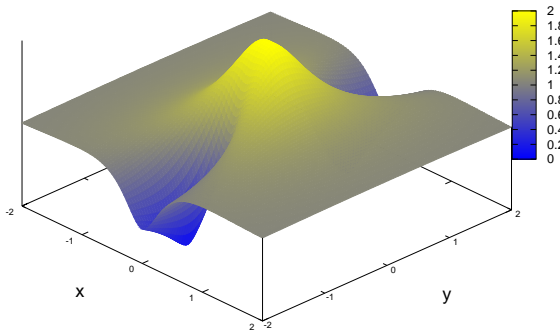
a.



b.



c.



d.

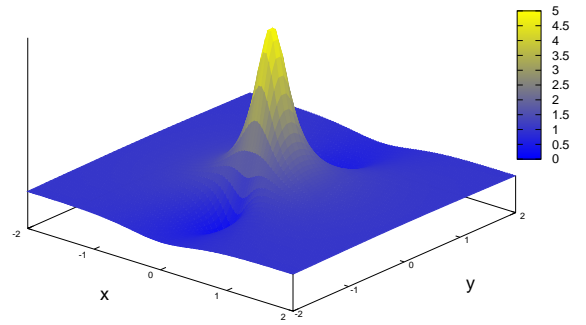


FIG 4. Full grown 2D rogue wave modelled by the modulus ($|q_{P(2D)}|$) of the static lump-solution (12) with different shapes and sizes, generated from the same single-peak solution. The maximum amplitude and modular inclination are tunable through two free parameters c and α showing: (a) High amplitude: 12 and high modular inclination, for $c = 1/13$, $\alpha = 4.0$. (b) High amplitude: 12 but low modular inclination, for $c = 1/13$, $\alpha = 0.4$. (c) Low amplitude: 2 and low modular inclination, for $c = 1/3$, $\alpha = 0.4$. (d) Moderate amplitude: 5 and moderate modular inclination, for $c = 1/6$, $\alpha = 1.2$. The last situation is the same as Fig. 5(c), obtained at $t = 0$.

3.2. Rogue wave with adjustable amplitude, inclination and hole waves

Note, that the static lump soliton (19), can be obtained from the dynamical RW solution (4) at the static point $t = 0$ (Fig. 5c) similar to static PB profile obtained from (3), and hence it physically represents a full grown RW solution as shown in Fig. 4 (d). Looking more closely into solution (12), for understanding the physical relevance of its free parameters c and α , we notice that the wave attains its maximum amplitude: $|q_{P(2D)}(0, 0)| \equiv A_{rog}(c) = (\frac{1}{c} - 1)$, at the center ($x = 0, y = 0$), while at large distances ($|x| \rightarrow \infty, |y| \rightarrow \infty$) the wave goes to the background plane wave, with its amplitude decreasing to $A_\infty = 1$. Therefore the maximum amplitude reachable by our RW solution, relative to that of the background wave is $\frac{A_{rog}(c)}{A_\infty} = (\frac{1}{c} - 1)$. Consequently, the amplitude of the full grown RW described by the lump soliton can be changed continuously by changing parameter c (with $A_{rogue}(c)$ increasing with decreasing c) and could therefore be adjusted to fit the heights of any observed RW. Consequently, the maximum RW amplitude in our model can be made as high as desired, by decreasing the value of an arbitrary smooth parameter c (see Fig. 4 (a-d), for particular examples). Comparing this situation with the conventional 1D RW model given by the PB (2) and its generalizations [22], as mentioned above, we conclude that, in the well known class of PB solutions, the maximum amplitudes reachable by the 1D RW are given by the fixed discrete odd numbers $2j + 1$, with $j = 1, 2, 3, \dots$ and can be obtained by going only to different higher solutions involving more and more complicated higher order polynomials. The higher rational solutions having free parameters [23, 24] become parameterless for a single-peak RW solution [24]. On the other hand, in our 2D RW model the maximum amplitude $A_{rog}(c)$ can be varied continuously and increased as required, by tuning an arbitrary parameter c in the same single-peak, first order solution (12) or its dynamical extension (19) (as shown in Fig. 4 (a-d)), making the model suitable for RWs with a diverse range of heights, anywhere in the range 17-30 meters in calm sea [2]-[4], as observed in deep sea 2D RWs.

Extending the modular inclination in case of 1D: $S_P^x(x)$, as defined in (5) we get for the full grown 2D RW solution (12) the modular inclination as

$$S_{P(2D)}^x(x, y) = \frac{\partial}{\partial x} |q_{P(2D)}(x, y)|, \quad S_{P(2D)}^y(x, y) = \frac{\partial}{\partial y} |q_{P(2D)}(x, y)| \quad (14)$$

Focussing on the inclination $S_{P(2D)}^x(x, 0)$ as observed at the middle of the wave front, we notice, that it is linked also to another free parameter α and attains its maximum

$$S_{P(2D)max}^x(x_m, 0) = -2\alpha x_m G^2(x_m, 0) \quad (15)$$

at $x_m = \frac{\sqrt{c}}{\sqrt{3\alpha}}$ with function $G(x, y)$ as defined in (12). We see that the maximum modular inclination of a full grown 2D RW in our model depends on both the parameters c and α in an intricate way and can be changed continuously by varying two arbitrary parameters to fit varied situations (Fig. 4(a-d)). Note that this inclination will be influenced by the physical steepness of the wave, contributing from the wave vector of the carrier wave. We can identify another intriguing feature of our solution, by noting that the amplitude of the wave (13) falls to its minimum: $A_0 = 0$, at $y = 0, x = \pm x_0$ where $x_0 = \sqrt{\frac{1}{\alpha}(1 - c)}$, which depends again on two free parameters. This significant feature emerging from our RW model, as will be demonstrated below in Fig. 5(a,b), is related to the *hole-wave* formation observed during ocean RWs [25, 26].

3.3. Topological consideration

Though the static lump-solution (12) can describe the profile of a full grown 2D RW, for modelling an evolving realistic RW, we need to find a time-dependent solution, which would smoothly go to its static form (12) at the moment $t = 0$. Our next aim therefore is to construct a dynamical lump soliton out of the static lump-solution, to create a true picture of a RW which can appear and disappear fast with time. However, for constructing such a solution we have to clarify first, whether it is possible in principle for our lump soliton to disappear without a trace, i.e. whether the soliton is free from all topological restrictions, which otherwise would prevent such a vanishing.

The reason for such suspicion is due an interesting lesson from topology stating that, when a complex field $q(x, y)$ is defined on a 2D space with non-vanishing boundary condition $|q| \rightarrow 1$ at large distances, but having vanishing values $q \rightarrow 0$ close to the center, we can define a unit vector $\hat{\phi} = \frac{q}{|q|}$ on an 1-sphere S^1 . However, this vector $\hat{\phi} = (\phi^1, \phi^2)$ is well defined only at the space boundaries: $\partial R^2 \sim S^1$ (since $q = 0$ at inner points), realizing a smooth map: $S^1 \rightarrow S^1$ with possible nontrivial topological charge $Q = n$. This charge with integer values $n = 0, 1, 2, \dots$, labels the distinct homotopy classes and is defined as the degree of the map, which unlike a Nöther charge is conserved irrespective of the dynamics of the system. Such a situation occurs for example in type II superconductors with the charge linked to the quantized flux of vortices for the magnetic field $\mathbf{B}(x, y)$ [37] :

$$2\pi Q = \int d\mathbf{S} \cdot \mathbf{B} = \int_C d\mathbf{l} \cdot \mathbf{A}, \quad (16)$$

where $\mathbf{B} = \text{curl } \mathbf{A} = \hat{\mathbf{z}}(\partial_x \phi^1 \partial_y \phi^2 - \partial_x \phi^2 \partial_y \phi^1)$. Notice that, our complex field solution $q_{P(2d)}(x, y)$ possesses clearly the features of $\hat{\phi}$ discussed above, since (12) goes to a constant modulation $-e^{4iy}$ at large distances and vanishes at points $(0, \pm x_0)$. Note that, such a solution related to a sphere to sphere map can not go to a trivial configuration, if it belongs to a homotopy class with nontrivial topological charge: $Q = n, n = 1, 2, 3, \dots$, due to conservation of the charge, with the only exception for the class with zero charge $Q = 0$. Therefore, for confirming the possible appearance/disappearance property of a RW for solution (12), we have to establish first that in spite of defining a nontrivial topological map, it belongs nevertheless to the sector with topological charge: $Q = 0$, i.e. our lump soliton is indeed shrinkable to the *vacuum* solution. For this we calculate explicitly the topological charge (16) associated with (12) as

$$2\pi Q = \int_C d\mathbf{l} \cdot \mathbf{A} = \int (dx A_x + dy A_y), \quad (17)$$

where $A_a = \phi^1 \partial_a \phi^2$, $\phi_1 = \text{Re } q/|q|$, $\phi_2 = \text{Im } q/|q|$, where the contour integral along x and y are taken along a closed square at the boundaries of the plane. Substituting explicit form of solution $q(x, y)$ from (12) and arguing about the oddness and evenness of the integrand with respect to x, y or checking directly by any analytic computational package one can show that the related charge is indeed $Q = 0$ and therefore the solution belongs to the trivial topological sector as we wanted. The intriguing reason behind this fact is that, the two holes appearing here have opposite charges resulting to their combined charge being zero.

3.4. Construction of dynamical lump soliton

For constructing a dynamical extension of the 2D static lump soliton (12) we realize that, a sudden change of amplitude with time, as necessary to mimic the 2D RW behavior, might result to a non-conservation of energy. This however can not be described by an integrable equation alone, since the integrability demands a strict conservation of all charges and therefore our integrable equation (8) needs certain modification for allowing the appearing/disappearing nature of its lump-solution. On the other hand, the importance of ocean currents in the formation of RWs is documented and repeatedly emphasized [4, 18, 26], which however is absent in equation (8). This motivates us to solve both these problems in one go, by modifying equation (8) with the inclusion of the effect of an *ocean current*, as in [4], by adding a term in the form $I = -iU_c q_x$. For obtaining an exact dynamical RW solution to the modified 2D NLS equation, we choose the current flowing along longitudinal directions and changing with time and location as $U_c(x, t) = \frac{\mu t}{\alpha x}$. Looking closely into the structure of this current term for the RW solution (19):

$$I(x, y, t) = i\left(\frac{\mu t}{\alpha x}\right) \frac{\partial}{\partial x} [q_{P(2D)}(x, y, t)] = -2\mu t(4y - i)G^2 e^{4iy}, \quad (18)$$

with G as defined in (19), it becomes apparent, that the currents would flow to the center of formation of the RW ($x = y = 0$) from both of the longitudinal and the trasverse sides, though with a directional preference, with their magnitude $|I(x, y, t)|$ increasing as they approach to the center, however stopping completely at the moment of the full surge at $t = 0$. The picture gets reversed after the RW event with currents flowing back quickly, away from

the center with the intensity of the current $|I|$ diminishing as the distance increases. Such an inflow and outflow of energy seems to be physically consistent with the formation of a 2D ocean RW. Note that, though the current factor U_c looks ill-defined, the multiplicative factor q_x makes the term $I(x, y, t)$ well-behaved on the RW solution (19), with the ocean current term becoming a smooth and bounded function in all space and time variables, as evident from (18). It has been suspected in earlier studies, that spatially nonuniform current should be responsible in the development of ocean rogue waves [18]. Such a nonuniform dependence on space variables can be seen in our current term $I(x, y, t)$. Interestingly, the modified 2D NLS equation ((8) with the inclusion of the current term I) admits now an exact dynamical 2D extension of the Peregrine soliton in the analytic form, though the modified equation loses its integrability in the sense, discussed in sect. 4.2. The dynamical RW solution has a similar form as (12), only with the function G becoming dynamical by the inclusion of time variable :

$$q_{P(2d)}(x, y, t) = e^{4iy}[-1 + (1 - i4y)G],$$

$$G \equiv \frac{1}{F(x, y, t)}, F(x, y, t) = \alpha x^2 + 4y^2 + \mu t^2 + c. \quad (19)$$

The arbitrary parameter μ appearing in the solution (19) is related to the ocean current and can control how fast the RW would appear and how long it would stay. Note again that (19) at $t = 0$, representing a full grown RW (see Fig 5c)) coinciding with the exact static lump-solution (12) of the 2D NLS equation (8) (as in Fig. 4d)), justifying the physical relevance of the static lump solution. At this stage, a comparison between 1D PB soliton

$$q_P(x, t) = [-1 + \frac{(1 - 4it)}{x^2 + 4t^2 + \frac{1}{4}}]e^{-2it} \quad (20)$$

and our 2D lump soliton

$$q_{P(2D)}(x, 0, t) = [-1 + \frac{(1)}{\alpha x^2 + \mu t^2 + c}], \text{ at } y = 0, \quad (21)$$

might be interesting. This shows that though there is some similarity between these two solutions, there are many differences as well at $y = 0$. In the absence of the transverse coordinate, the 2D solution (21) of our modified equation, becomes real, though still having 3 independent free parameters. The 1D PB soliton on the other hand is complex with a breathing mode, but without any free parameter.

We should mention here, that the 2D extension of PB solution (19), unlike the standard 1D PB, unfortunately could not be derived as a limiting case from the breather solution of 2D NLS equation (8), due to the two-dimensional nature of the solution and has to be constructed by direct insertion through an ansatz.

3.5. Proposed 2D rogue wave model and its dynamics

It is convincingly demonstrated in Fig. 5 (fixing the free parameters to certain values), how the envelop wave $|q_{P(2D)}(x, y, t)|$ corresponding to the exact dynamical 2D lump-soliton (19), dependent on time t and two space variables x and y on a plane, evolves from a background plane wave existing in the distance past and how it could acquire a sudden 2D hole at the centre ($x = 0, y = 0$) at the moment $t_h = -\sqrt{\frac{1}{\mu}(1 - c)}$, ($t_h = -0.83$ for $c = 1/6, \mu = 1.2$ in Fig. 5a), as told in marine-lore [5, 15, 25]. The hole subsequently splits into two and shift apart from the centre (Fig. 5b)), to make space for a high steep upsurge of the lump forming the full grown RW (Fig. 5c) at time $t = 0$. Note that we have derived analytically the exact positions of these holes in sect. 3.2. With the passage of time the picture gets reversed and the 2D RW disappears fast into the background waves with the 2D holes merging at the centre and vanishing again. Thus our model describes vividly well the reported picture of the ocean surface RWs [4, 13, 26] as well as those found in large scale 2D experiments [8]. Since our model is an exact one, we could work out these details analytically. The surface RWs modelled by our solution (19) and as visible from Fig. 5 (similarly from solution (12) and Fig. 4), shows a distinct directional preference and an asymmetry between the two space variables x, y , (similar to the report of [4, 13]). The maximum amplitude attained by the full grown RW (as shown in Fig 5c)

is five-times that of the background waves, due to our choice $c = 1/6$. Examples of other amplitudes and modular inclination of full grown RWs for some other choices of the free parameters c and α , as modelled by the static solution (12), are presented already in Fig. 4 (a-d).

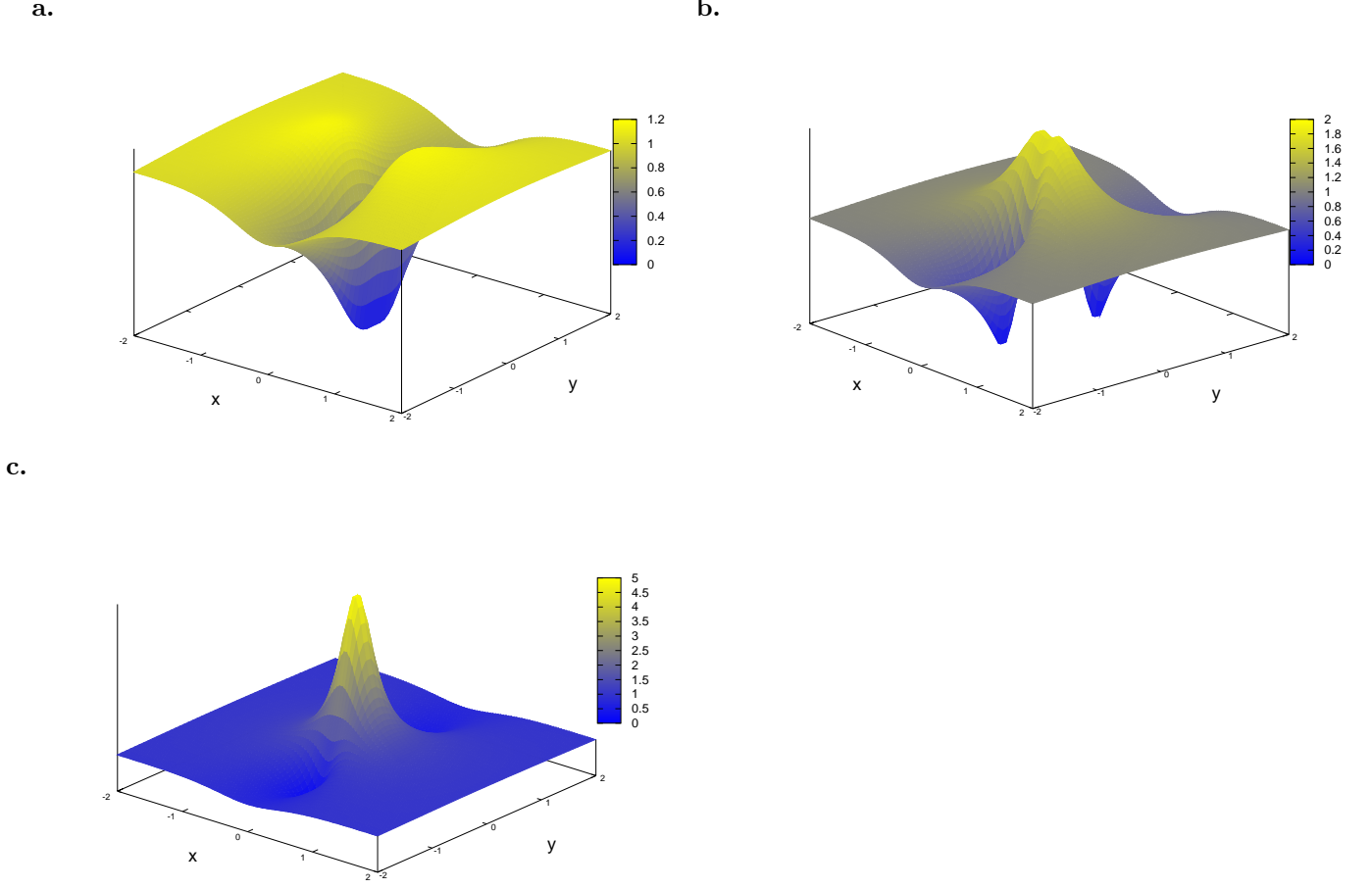


FIG 5. Snap shots of a 2D rogue wave with 2D holes during its formation at different time, described by the modulus $|q_{P(2D)}(x, y, t)|$ of the dynamical lump-soliton (19) with parameter values $c = 1/6$, $\alpha = 1.2$ and $\mu = 1.2$, at three crucial moments of time: (a) At $t = t_h = -0.83$: Creation of a 2D hole at the centre. (b) At $t = -0.40$: The hole splits into two are drifting away from the centre. (c) At $t = 0.0$: The full grown RW, corresponds also to the static lump solution (12), as shown in Fig. 4(d).

4. PHYSICAL ORIGIN OF THE PROPOSED 2D NLS EQUATION AND ITS INTEGRABILITY

We have shown that the 2D NLS equation (8) which is equivalent to nonlinear equation (7) can give an exact model, considerably successful in describing realistic 2D rogue waves. In this section we show the direct link of the 2D NLS equation with basic hydrodynamic equations. Moreover we show the underlying integrable structures of the proposed equation.

4.1. Derivation of the integrable 2D NLS equation from basic hydrodynamic equations

For emphasizing the physical significance of our main nonlinear integrable equation (8), on which the ocean rogue wave model is based, we show its direct link with basic hydrodynamic equations. The procedure is based on a multi-scale expansion, at par with the celebrated equations like KdV, NLS etc [36, 49], though one should include here an

extra space dimension with an asymmetric scaling in space variables, considering the perturbative expansion to the next higher order. This is consistent however with the modelling of an ocean rogue wave, which is a surface phenomena with a likely broken space symmetry and directional preference [9]. Before entering into the detailed calculation, three dimensionless entities: $\epsilon = \frac{a}{h_0}$, $\delta = \frac{h_0}{\lambda_x}$ and $\mu = \frac{\lambda_x}{\lambda_y}$ are defined where a is the maximum amplitude, h_0 is the constant water depth, λ_x and λ_y are the wavelengths of the surface wave along longitudinal and transverse directions. The nonlinear parameter ϵ is responsible for the slow evolution of a harmonic wave of wavenumber k_x, k_y . The wave is thus slowly modulated as ϵ tends to 0 and therefore this small parameter can be used for perturbative expansion. Smallness of ϵ is consistent with the deep water limit with $a \ll h_0$ and hence with the formation of oceanic rogue waves. Note that parameters ϵ and δ are similar to those appearing in the derivation of the well known 1D NLS equation, with ϵ small and δ without any restriction, as also true in our case. However, an additional parameter μ , also without any restriction on its value appears in our 2D case, due to the presence of an additional transverse direction.

The first step in the derivation is to write the basic hydrodynamic equations for inviscid, irrotational and incompressible fluid in dimensionless variables, for the velocity potential field $\phi(t, x, y)$ and the gravity wave $\eta(t, x, y)$ as the free surface displacement above the mean water depth h_0 in the form

$$\phi_{zz} + \delta^2(\phi_{xx} + \mu^2\phi_{yy}) = 0, \quad (22)$$

at $0 < z < 1 + \epsilon\eta$, which comes from continuity equation. The equation

$$\phi_z = \delta^2[\eta_t + \epsilon(\phi_x\eta_x + \mu^2\phi_y\eta_y)], \quad (23)$$

called kinematic condition, is valid on $z = 1 + \epsilon\eta$. The equation

$$\phi_t + \eta + \frac{1}{2}\epsilon[\frac{\phi_z^2}{\delta^2} + \phi_x^2 + \mu^2\phi_y^2] = 0 \quad (24)$$

is the Bernoulli's equation and also valid at $z = 1 + \epsilon\eta$, while

$$\phi_z = 0 \quad (25)$$

is the fixed boundary condition valid at $z = 0$, i.e. at the bottom.

We introduce new variables with different scaling through ϵ as

$$\xi = k_x x + k_y y - \omega t, \quad \zeta = \epsilon(x - M_x t), \quad Y = \epsilon^2 y, \quad \tau = \epsilon^3 t, \quad (26)$$

where ω, M_x are frequency and velocity parameters to be determined later. Note, that the two space variables are treated with a non-symmetric scaling and using these set of variables, equations (22 -25) become

$$\phi_{zz} + \delta^2(k_x^2\phi_{\xi\xi} + \epsilon^2\phi_{\zeta\zeta} + 2\epsilon k_x\phi_{\zeta\xi}) + \mu^2\delta^2(k_y^2\phi_{\xi\xi} + \epsilon^4\phi_{YY} + 2\epsilon^2 k_y\phi_{Y\xi}) = 0 \quad (27)$$

$$\phi_z = \delta^2[-\omega\eta_\xi - \epsilon M_x\eta_\zeta + \epsilon^3\eta_\tau] + \epsilon\delta^2(k_x\phi_\xi + \epsilon\phi_\zeta)(k_x\eta_\xi + \epsilon\eta_\zeta) + \mu^2\epsilon\delta^2(k_y\phi_\xi + \epsilon^2\phi_Y)(k_y\eta_\xi + \epsilon^2\eta_Y) \quad (28)$$

and

$$[-\omega\phi_\xi - \epsilon M_x\phi_\zeta + \epsilon^3\phi_\tau] + \eta + (\frac{\epsilon}{2\delta^2})\phi_z^2 + \frac{\epsilon}{2}(k_x\phi_\xi + \epsilon\phi_\zeta)^2 + \frac{\mu^2\epsilon}{2}(k_y\phi_\xi + \epsilon^2\phi_Y)^2 = 0 \quad (29)$$

both valid at $z = 1 + \epsilon\eta$, while

$$\phi_z = 0, \text{ at } z = 0. \quad (30)$$

Seeking asymptotic solution of these equations in the series form

$$\phi = \sum_{n=0}^{\infty} \epsilon^n \phi_n(\xi, \zeta, Y, \tau, z), \quad \eta = \sum_{n=0}^{\infty} \epsilon^n \eta_n(\xi, \zeta, Y, \tau) \quad (31)$$

and using this expansion of dependent variables along with the scaled independent variables, different sets of equations are obtained from the basic set (27)-(30) at different powers of ϵ . In each ϵ order different equations are obtained for various powers of E and E^* . We would consider these equations sequentially at each order of parameter ϵ .

1) ϵ^0 order : The solution of interest in this case takes the form

$$\phi_0 = f_0 + F_0 E + F_0^* E^*, \eta = A_0 E + A_0^* E^*, \quad (32)$$

where $F_0(\zeta, Y, \tau, z)$, $A_0(\zeta, Y, \tau)$ are complex functions with F_0^* , A_0^* as complex conjugates, while $f_0(\zeta, Y, \tau)$ is a real function and $E = \exp(i\xi)$.

Using (27) and (30), F_0 , can be determined as

$$F_0 = G_0 \cosh(\delta K_1 z), \text{ where } G_0 = \frac{-i A_0 \omega \delta}{K_1 \sinh(\delta K_1)}, K_1 = \sqrt{k_x^2 + \mu^2 k_y^2}. \quad (33)$$

Using other two nonlinear boundary conditions (28), (29) we obtain the dispersion relation $\omega^2 = \frac{K_1}{\delta} \tanh(\delta K_1)$

2) ϵ order : Expanding ϕ_n , η_n as

$$\phi_n = \sum_{m=0}^{n+1} F_{nm} E^m + c.c., \quad \eta_n = \sum_{m=0}^{n+1} A_{nm} E^m + c.c., \quad (34)$$

where $F_{nm}(\zeta, Y, \tau, z)$ and $A_{nm}(\zeta, Y, \tau)$ are to be determined for various powers of E , at each powers of ϵ .

At ϵ order, the components $F_{10}, F_{11}, F_{12}, A_{10}, A_{11}, A_{12}$ and the velocity parameter M_x are determined from the equations corresponding to E , E^2 and E^0 , explicit forms of which are appended in A11.

3) ϵ^2 order: At this order a NLS type equation (Space coordinate Y replacing the time coordinate) is obtained, collecting the coefficients of E from (28), (29) and by using the quantities, already determined. Before calculating the final form of this equation some other components namely $F_{21}, F_{20}, f_{0\zeta}$ at this order need to be evaluated, which are given in the appendix A22.

The final form of the NLS like equation is obtained eliminating the unknown terms and expressing other terms through the single function A_0 as

$$i\alpha_1 A_{0Y} + \alpha_2 A_{0\zeta\zeta} + \beta_2 |A_0|^2 A_0 = 0, \quad (35)$$

where the constant coefficients α_1 , α_2 and β_2 are also given in appendix A22

Following the same procedure the components $F_{22}, A_{22}, A_{20}, f_{0Y}$ are determined, which we are not furnishing here due to their cumbersome expressions.

4) ϵ^3 order: In this order an evolution equation is obtained, for which some relevant components i.e. F_{31}, F_{30} etc, are also determined by continuing with the same procedure. The explicit forms of these coefficients presented in A33.

The evolution equation obtained by using equation (28), (29) and collecting coefficients of E takes the form

$$iaA_{0\tau} + \alpha_{31} A_{0\zeta Y} + i\bar{\beta}_{32} A_0^2 A_{0\zeta}^* + i\bar{\beta}_{31} |A_0|^2 A_{0\zeta} + ieG_{11}^* A_0^2 + ifG_{11} |A_0|^2 + i\alpha_{32} A_{0\zeta\zeta} = 0, \quad (36)$$

where $a, \alpha_{31}, \bar{\beta}_{32}, \bar{\beta}_{31}, e, f, \alpha_{32}$ are real constants dependent on parameters k_x, k_y, μ, δ .

If it is assumed, that the term G_{11} depends also on A_0 like the other terms as $F_0 \sim A_0$ and $G_{12}, A_{12} \sim A_0^2$ etc. (see Appendix), then the only consistent relation would be $G_{11} = P_1 A_{0\zeta}$, where P_1 is a real constant, dependent only on k_x, k_y, μ, δ . Using this relation in (36) one simplifies it in the form

$$iaA_{0\tau} + \alpha_{31} A_{0\zeta Y} + i\alpha_{32} A_{0\zeta\zeta} + i(\beta_{31} |A_0|^2 A_{0\zeta} + \beta_{32} A_0^2 A_{0\zeta}^*) = 0, \quad (37)$$

where β_{31}, β_{32} , are another set of constant coefficients expressed through earlier coefficients. Notice that the above equation (37) is similar to but not the same as our integrable 2D NLS equation due to the appearance of the term $i\alpha_{32} A_{0\zeta\zeta}$. However fortunately we have another equation (35) at our disposal, obtained at a lower order. Taking derivative of (35) with respect to ζ we derive the relation

$$i\alpha_2 A_{0\zeta\zeta} = \alpha_1 A_{0\zeta Y} - i\beta_2 (|A_0|^2 A_0)_\zeta \quad (38)$$

using which we can eliminate this unwanted term from (37) to obtain an equation in the form

$$iC_0A_{0\tau} + C_1A_{0\zeta Y} + iC_2A_0(A_0A_{0\zeta}^* - A_0^*A_{0\zeta}) = 0, \quad (39)$$

under the condition on the coefficients of the original equation as

$$\frac{\beta_2}{\alpha_2} = \frac{(\beta_{32} + \beta_{31})}{3\alpha_{32}} \quad (40)$$

Rescaling ζ , Y and τ and renaming A_0 equation (39) goes directly to the 2D NLS equation (8), which is equivalent to (7) proposed by us. Note that constraint (40), we have to impose for deriving our integrable 2D NLS equation from the basic hydrodynamic equations, though does not hold for general water wave problems, this loss of generality is compensated for by the gain of our important exact results. This in general is true for all integrable models.

4.2. Integrable structures of the proposed equation:

We present here the associated integrability properties of equation (9). The one-soliton solution of this equation is given in the form $q_{s(2d)}(x, y, t) = \text{sech}\kappa(y + \rho x - vt)e^{i(k_1x + k_2y + \omega t)}$, while allowing also higher soliton solutions and infinite set of conserved quantities [35]. One can also find the associated linear system

$$\Phi_y = U(\lambda)\Phi, \Phi_t = V(\lambda)\Phi,$$

with a Lax pair given by

$$U(\lambda) \equiv V_2(\lambda) = 2\lambda V_1(\lambda) + V_2^{(0)}, \quad V(\lambda) \equiv V_3(\lambda) = 2\lambda V_2(\lambda) + V_3^{(0)} \quad (41)$$

where

$$\begin{aligned} V_1(\lambda) &= i(\lambda\sigma^3 + U^{(0)}), \quad V_2^{(0)} = \sigma^3(U_x^{(0)} - iU^{(0)^2}) \\ V_3^{(0)} &= -\sigma^3U_y^{(0)} - [U^{(0)}, U_x^{(0)}], \quad U^{(0)} = q\sigma^+ + q^*\sigma^-, \end{aligned} \quad (42)$$

with σ^a , $a = \pm, 3$, Pauli matrices, the flatness condition: $U_t - V_y + [U, V] = 0$, of which generates our 2D NLS equation (8). Note that unlike the known Lax pair of the 1D NLS, the pair $U(\lambda), V(\lambda)$ associated to our system have higher order dependence on the spectral parameter λ . It is not difficult to show, that the flatness condition yields from (42) different relations at different powers of λ . The equation linked to the λ corresponds to our $(2+1)$ -dimensional NLS equation (8), while the relation with λ^0 gives another intriguing nonlinear equation

$$iq_{xt} + q_{yy} + 2i|q|^2q_y + 2q_x(qq_x^* - q^*q_x) = 0. \quad (43)$$

Our main concern here however is the 2D NLS equation (8), which we intend to use for constructing a 2D rogue wave model. Note however, the modification of (8) by the addition of the current term as considered in the sect. 3.4, though yields exact analytic RW solution no longer remains integrable in the sense described here.

5. CONCLUDING REMARKS

We conclude by listing a few distinguishing features of our proposed dynamical lump soliton (19), which are important for a realistic ocean RW model.

- 1) This is the first 2D dynamical RW model given in an analytic form.
- 2) It is a 2D extension of Peregrine like soliton, representing an exact lump solution linked to a novel $(2+1)$ -dimensional integrable NLS equation, derivable from the basic hydrodynamic equations.
- 3) The dynamics of the RW solution is induced by a ocean current term and controlled by it. Importance of the current in the formation of RW is strongly emphasized [4, 8], though perhaps for the first time this effect in 2D is attempted to be analyzed analytically in our model.

4) Both the height and the inclination of the single peak RW are adjustable by two independent free parameters present of our model.

5) The fastness of appearance of the RW and the duration of its stay can be regulated by yet another parameter linked to the ocean current.

6) The proposed solution and MI exhibit broken spatial symmetry as well as a directional preference, which are suspected to be the crucial features in the formation of a 2D RW [8, 9, 14, 15]. Note again that these features obtained earlier through observation or numerical simulation, found and confirmed in our model through exact analytic result.

7) Strange appearance (and disappearance) of a 2D hole just before (and after) the formation of the rogue wave [15, 25, 26] is also confirmed in our model, graphically as well as by analytic findings.

In comparison the original Peregrine soliton (2) (together with its higher order solutions), by far the most popular model of the rogue wave, does not exhibit most of these essential properties, due to its inherently one-dimensional nature and absence of free parameters. Therefore, while the class of Peregrine solitons are successful in modelling 1D rogue wave like structures observed in many experiments, the two-dimensional rogue wave model reported here should complement it, to stand close to a realistic model for ocean surface rogue waves.

We hope that, this breakthrough in describing large ocean RWs by an analytic dynamical lump-soliton with adjustable height, inclination and duration would also be valuable for experimental findings of two-dimensional RWs in other systems like capillary fluid waves [11] optical cavity waves [9] and basin water waves [8]. Derivation of our exact lump soliton from the breather solution of the integrable 2D NLS equation presented here, in a systematic way as well as to find higher order rational lump solutions would be challenging theoretical problems.

ACKNOWLEDGEMENT

A.K. thanks P. Mitra for valuable discussions and the AvH Foundation for support.

* Electronic address: anjan.kundu@saha.ac.in

† Electronic address: abhik.mukherjee@saha.ac.in

‡ Electronic address: tnaskar@gmail.com

- [1] <http://news.bbc.co.uk/2/hi/8548547.stm>
- [2] C. Kharif & E. Pelinovsky *Eur. J. Mech.* B -Fluid **22** (2003) 603; K. Dysthe, H. E. Krogstad & P. Muller *Annu. Rev. Fluid Mech.* **40** (2008) 287; C. Kharif C, E. Pelinovsky & A. Slunyaev *Rogue waves in Ocean* (Springer-Verlag, Berlin Heidelberg, 2009) (with references therein); A. R. Osborne *Nonlinear Ocean waves and the inverse scattering transform*, Int. Geophys. Ser. **97** (Acad. Press, 2010).
- [3] C. Bonatto et al. *Phys. Rev. Lett.* **107** (2011) 053901.
- [4] M. Onorato, D. Proment & A. Toffoli *Phys. Rev. Lett.* **107** (2011) 184502 (and references therein).
- [5] V. E. Zakharov, A. I. Dyachenkov & R. V. Shamin *Eur. Phys. J. Special Topics* **185** (2010) 113124
- [6] D. R. Solli, C. Ropers, P. Koonath, B. Jalali *Nature* **450** (2007) 06402
- [7] A. N. Ganshin et al *Phys. Rev. Lett.* **101** (2008) 065303
- [8] M. Onorato et al *Phys. Rev. Lett.* **102** (2009) 114502
- [9] A. Montina, et al *Phys. Rev. Lett.* **103** (2009) 173901.
- [10] Kibler B, et al. *Nature Physics* **6** (2010) 790.
- [11] M. Shats, H. Punzmann, & H. Xia *Phys. Rev. Lett.* **104** (2010) 104503.
- [12] A. Chabchoub, N. P. Hoffmann & N. Akhmediev *Phys. Rev. Lett.* **106** (2011) 204502.
- [13] A. N. Pisarchik, et al *Phys. Rev. Lett.* **107** (2011) 274101.
- [14] B. Eliasson, & P. K. Shukla *Phys. Rev. Lett.* **105** (2010) 014501.
- [15] A. R. Osborne, M. Onorato & M. Serio *Phys. Lett. A* **275** (2000) 386.
- [16] M. J. Ablowitz, J. Hammack, D. Henderson & C. M. Schober *Phys. Rev. Lett.* **84** (2000) 887.
- [17] N. Akhmediev & E. Pelinovsky *Eur. Phys. J. Special Topics* **185** (2010) 1.
- [18] V. P. Ruban *Phys. Rev. Lett.* **99** (2007) 044502.
- [19] D. H. Peregrine *Austral. Math. Soc. B* 25 (1983) 16.
- [20] M. Lakshmanan in *Tsunami and Nonlinear Waves* (Ed. A. Kundu, Springer Verlag, NY, 2006) p. 31

- [21] G. P. Agarwal *Nonlinear fiber optics* (Acad. Press, London, 2007), ch. 5.
- [22] N. Akhmediev, A. Ankiewicz & J. M. Soto-Crespo *Phys. Rev. E* **80**(2009) 026601.
- [23] P. Dubard & V. B. Matveev *Nat. Hazards Earth Syst. Sci.* **11**(2011) 667.
- [24] A. Ankiewicz, D.J. Kedziora & N. Akhmediev *Phys. Lett. A* **375** (2011) 2782.
- [25] http://wikipedia.org/wiki/Rogue_wave
- [26] A. I. Dyachenko & V. E. Zakharov *JETP Lett.* **81** (2005) 6.
- [27] M. Ablowitz & H. Segur *Solitons and the Inverse Scattering Transform*, (SIAM, Philadelphia, 1981).
- [28] A. Calini & C. M. Schober *Phys. Lett. A* **298** (2002) 335349.
- [29] Y. C. Ma *Stud. Appl. Math.* **60** (1979) 43.
- [30] N. N. Akhmediev, V. M. Eleonskii & N. E. Kulagin *Theor. Math. Phys.* **72** (1987) 809.
- [31] <http://news.bbc.co.uk/2/hi/3917539.stm>
- [32] <http://earthobservatory.nasa.gov/IOTD/view.php?id=44567>
- [33] K. B. Dysthe & K. Trulsen *Phys. Scr.* **82** (1999) 48.
- [34] Y. Ohta & J. Yang, arXiv: 1206.2548 [nlin.SI], (2012)
- [35] A. Kundu, arXiv: 1201.0627 [nlin.SI], (2012) A. Kundu & A. Mukherjee, arXiv:1305.4023 [nlin.SI] (2013).
- [36] R. S. Johnson *A Modern Introduction to the Mathematical Theory of Water Waves*, (Cambridge Texts in Appl. Math., 2004).
- [37] Z. Parsa *Am. J. Phys.* **47** (1979) 56.
- [38] J.W McLean *J.Fluid Mech* **114** (1982) 331.
- [39] C. Kharif & A. Ramamonjiarisoa *Phys.Fluids* **31** (1988) 1286.
- [40] T.B Benjamin & J.E. Feir *J.Fluid Mech* **27** (1967) 417.
- [41] K.B.Dysthe *Proc.R.Soc.Lond.A* **369** (1979) 105.
- [42] Y. Ohta & J. Yang *J.Phys A:Math. Theor.* **46** (2013) 105202.
- [43] M. Boiti, J. Leon & F. Pempinelli *Inv. Prob.* **3** (1987) 37.
- [44] E. Infeld, A.Senatorski & A.A. Skorupski *Phys. Rev. E.* **51** (1995) 4.
- [45] A.Davey & K. Stewartson *Proc.R.Soc.Lond.A* **338** (1974) 101.
- [46] V. E. Zakharov, in *Solitons* (Ed. R. K. Bullough and P. J. Caudrey, Springer, Berlin, 1980)
- [47] V. E. Zakharov *JETP Lett.* **35** (1972) 908.
- [48] G. Mu, Z.Dai & Z. Zhao *Pramana J. Phys.* **81** 3, (2013) 367 .
- [49] M. J. Ablowitz *Nonlinear Dispersive waves, Asymptotic Analysis and Solitons*, (Cambridge University Press. 2011).

APPENDIX:

A11: Coefficients appearing in order ϵ :

$$\begin{aligned}
 F_{10} &= G_{10}(\zeta, Y, \tau), \quad A_{10} = M_x f_{0\zeta} - \frac{2\delta K_1}{\sinh(2\delta K_1)} |A_0|^2 \\
 F_{12} &= G_{12} \cosh(2\delta K_1 z), \text{ where } G_{12} = \frac{-3i\omega\delta^2}{4\sinh^4(\delta K_1)} A_0^2, \\
 A_{12} &= \frac{\delta K_1 \cosh(\delta K_1)}{2[\sinh(\delta K_1)]^3} [1 + 2\cosh^2(\delta K_1)] A_0^2 \\
 F_{11} &= G_{11} \cosh(\delta K_1 z) - \frac{i\delta k_x}{K_1} G_{0\zeta} z \sinh(\delta K_1 z), \\
 A_{11} &= i\omega [G_{11} \cosh(\delta K_1) - \frac{i\delta k_x}{K_1} G_{0\zeta} \sinh(\delta K_1)] + M_x [G_{0\zeta} \cosh(\delta K_1)] \\
 \text{The velocity parameter: } M_x &= \frac{\omega k_x}{2K_1^2} [1 + \frac{2\delta K_1}{\sinh(2\delta K_1)}]
 \end{aligned}$$

A22: Coefficients appearing in order ϵ^2 :

$$\begin{aligned}
 F_{21} &= G_{21} \cosh(\delta K_1 z) - \frac{i\delta k_x}{K_1} G_{11\zeta} z \sinh(\delta K_1 z) - \frac{i\delta k_y}{K_1} \mu^2 G_{0Y} z \sinh(\delta K_1 z) + G_{0\zeta\zeta} [(-\frac{\delta}{2K_1}) z \sinh(\delta K_1 z) + \\
 &(\frac{\delta k_x^2}{2K_1^2}) z \sinh(\delta K_1 z) - (\frac{\delta^2 k_x^2}{2K_1^2}) z^2 \cosh(\delta K_1 z)], \\
 f_{0\zeta} &= \frac{1}{(1-M_x^2)} [-\frac{2M_x \delta K_1}{\sinh(2\delta K_1)} - \frac{2\omega \delta k_x \coth(\delta K_1)}{K_1}] |A_0|^2, \\
 F_{20} &= -\delta^2 f_{0\zeta\zeta} \frac{z^2}{2} + G_{10}(\zeta, Y, \tau), \\
 \alpha_1 &= -k_y \mu^2 \tanh(K_1 \delta) \frac{[2K_1 \delta + \sinh(2K_1 \delta)]}{2\omega^3 \cosh^2(K_1 \delta)}, \\
 \alpha_2 &= \frac{\delta}{2\omega K_1^3} [K_1^3 \delta \{2M_x^2 - \frac{1}{\cosh^2(K_1 \delta)}\} - K_1^2 \tanh(K_1 \delta) + k_x^2 \tanh(K_1 \delta) + 4K_1 k_x M_x \delta^3 \omega^3 - K_1 k_x^2 \delta \{1 + \tanh^2(K_1 \delta)\}], \\
 \beta_2 &= -\frac{\delta^2}{\omega(1-M_x^2)} [4k_x^2 + K_1 \delta \frac{1}{\sinh(2K_1 \delta)} \{K_1^2 ((-1 + M_x^2)(8 + \cosh(4K_1 \delta) \frac{1}{\sinh^2(K_1 \delta)} + 2 \frac{1}{\cosh^2(K_1 \delta)}) + 8k_x M_x \omega\}]
 \end{aligned}$$

A33: Coefficients appearing in order ϵ^3 :

$$F_{30} = -\delta^2 F_{10\zeta\zeta} \frac{z^2}{2} + G_{30}(\zeta, Y, \tau), \quad (44)$$

$$\begin{aligned} F_{31} = & G_{31} \cosh(\delta K_1 z) + G_{21\zeta} \left\{ \left(\frac{-i\delta k_x}{K_1} \right) z \sinh(\delta K_1 z) \right\} + G_{11\zeta\zeta} \left\{ \left(\frac{i\delta k_x}{K_1} \right)^2 \frac{z^2}{2} \cosh(\delta K_1 z) - \left(\frac{i\delta k_x}{K_1} \right)^2 \left(\frac{z}{2\delta K_1} \right) \sinh(\delta K_1 z) - \right. \\ & \left. \left(\frac{\delta}{2K_1} \right) z \sinh(\delta K_1 z) \right\} + \left(\frac{i\delta k_x}{K_1} \right) G_{0\zeta\zeta\zeta} \left\{ \left(\frac{\delta}{2K_1} \right) (z^2/2) \cosh(\delta K_1 z) - \left(\frac{\delta}{2K_1} \right) \left(\frac{z}{2\delta K_1} \right) \sinh(\delta K_1 z) - \left(\frac{\delta k_x^2}{2K_1^3} \right) \frac{z^2}{2} \cosh(\delta K_1 z) + \right. \\ & \left. \frac{\delta k_x^2}{2K_1^3} (z/2\delta K_1) \sinh(\delta K_1 z) + \left(\frac{\delta}{2K_1} \right) \frac{z^2}{2} \cosh(\delta K_1 z) - \left(\frac{\delta}{2K_1} \right) \left(\frac{z}{2\delta K_1} \right) \sinh(\delta K_1 z) + \frac{\delta^2 k_x^2}{2K_1^2} \frac{z^3}{3} \sinh(\delta K_1 z) - \right. \\ & \left. \frac{\delta^2 k_x^2}{2K_1^2} (z^2/2\delta K_1) \cosh(\delta K_1 z) + \frac{\delta^2 k_x^2}{2K_1^2} (z/2\delta^2 K_1^2) \sinh(\delta K_1 z) \right\} + G_{0\zeta Y} \left(\frac{i\delta k_x}{K_1} \right) \left(\frac{i\delta k_y}{K_1} \right) [\mu^2 z^2 \cosh(\delta K_1 z) - \\ & \mu^2 \sinh(\delta K_1 z) \left(\frac{z}{\delta K_1} \right)] + G_{11Y} \left[- \left(\frac{i\delta k_y}{K_1} \right) \mu^2 z \sinh(\delta K_1 z) \right] \end{aligned}$$